IJMECIE

International Journal of Mechanical, Electrical and Civil Engineering

E-ISSN: 3047-4531
P-ISSN: 3047-4523

Research Article

Performance Study of the Francis Turbine Runner at Tanggari I Hydroelectric Power Plant via CFD and Reverse Engineering

Achmad Walid [1,*], Irwanda Yuni Pungkiarto [2]

[1] Mechanical Engineering Department, Politeknik Negeri Malang, Malang Indonesia : achmad.walid@polinema.ac.id
[2] Mechanical Engineering Department, Politeknik Negeri Malang, Malang Indonesia : irwanda.yp@polinema.ac.id
* Corresponding Author : Achmad Walid

Abstract: This study aims to analyze the performance and conduct reverse engineering of the Francis Turbine runner at the Tanggari 1 Hydroelectric Power Plant (PLTA Tanggari 1) through 3D scanning and Computational Fluid Dynamics (CFD) simulation. The main objective is to evaluate the turbine's efficiency and identify areas for improvement in the runner geometry. Data from the 3D scan are used to reconstruct a CAD model, which is then numerically tested to predict hydraulic performance. CFD simulations are carried out under various guide vane openings and head variations. The simulation results show a maximum efficiency of 93% at a head of 122.4 meters with a guide vane opening angle of 26° and a flow rate of 8.5 m^3/s. The resulting performance curve and hill chart indicate the optimal operating point or Best Efficiency Point (BEP), which serves as a critical reference for turbine operation settings. Flow phenomena such as separation and vortex formation were detected under off-BEP operating conditions, potentially causing pressure fluctuations and vibrations. As a technical recommendation, it is advised to operate the turbine close to the BEP to minimize vibrations and energy losses. Furthermore, the runner geometry obtained from reverse engineering can serve as a basis for component refabrication and the development of new runner designs that are more adaptive to varying load conditions.

Keywords: BEP; CFD; Francis Turbine; Guide Vane; Runner

1. Introduction

With a large part of global energy needs expected to be fulfilled by renewable sources, hydropower has remained the most dependable option since its inception [25]. From the 1950s to the present, Computational Fluid Dynamics (CFD) has evolved into one of the most reliable design methods. In practical turbomachinery design, turbine blades are often geometrically complex and take the form of freeform surfaces, leading to twisted blade shapes [17]. CFD enables the prediction of fluid flow within complex domains and provides an efficient way to visualize key turbine parameters that significantly influence the performance of hydro turbines [1]. For decades, it has been utilized to analyze flow within hydraulic turbines. Numerical modeling presents a challenge because the specialized modeling approaches used to investigate specific operating conditions often do not complement each other, while multiple flow phenomena may occur simultaneously [2].

CFD simulations as well as model tests examining the correlation between flow patterns and hydraulic losses in pump turbines functioning in pump mode revealed a pressure drop at low-pressure flow rates, attributed to hydraulic losses at the rotor-stator interface. These findings suggest that hydraulic failures in the flow path are the main cause of pressure fluctuations [3]. Numerous traditional hydraulic turbines, including Francis, Kaplan, Pelton, and Propeller turbines, have been engineered as well as optimized to efficiently fulfill energy needs [4].

Received: May 30, 2025;
Revised: June 30, 2025;
Accepted: July 12,2025;
Published : July 14, 2025
Curr. Ver.: July 14, 2025

The CFD methodology has been employed to examine unsteady swirling vortices in the Francis turbines' draft tube operating beneath partial load states, complemented by experimental studies on the same flow phenomena [5]. Obrovsky et al. (2013) also showed the design process for high-speed turbines, utilizing CFD and applying automatic optimization methods in runner design to evaluate the influence of different runner parameters on the performance, as well as the hydraulic turbines' cavitation characteristics [6].

Previous studies have shown that more than 60% of installed turbines, along with nearly 80% of hydro turbines needed for forthcoming installations, such as those in the Himalayan basin in Nepal, will require Francis-type turbines [7]. Hydroelectric power plants with Francis turbines function by transforming the water's potential and kinetic energy into mechanical energy as the runner blades rotation, which is subsequently transformed into electrical energy by a generator. These turbines are typically employed in medium to high head applications, ranging from 20 to 600 meters, and can operate with high efficiency levels of around 90–95%. In this system, water flows through a spiral casing and guide vanes that regulate the flow before it strikes the runner, enabling the shaft connected to the generator to rotate.

The Francis turbine is the most commonly utilized worldwide, known for its compact design, excellent operational efficiency, and ability to function across a wide spectrum of water heads. Typically, this turbine operates effectively with water heads between 100 and 300 meters, allowing it to reach optimal energy conversion efficiencies of 90–95% [8]. The flow conditions entering the Francis turbine runner blades greatly affect the turbine's performance. Changes in velocity and pressure can create flow instability within the turbine. If the instability is strong enough, it will cause significant pressure fluctuations [9].

The Francis turbine's final component is the draft tube, a channel that joins the runner to the tailwater. Due to its geometric design, the draft tube allows for a gradual increase in water pressure along the tube, thereby maximizing pressure recovery [10]. The geometry of the turbine runner is complex and influenced by multiple design parameters [1].

Tanggari 1 Hydroelectric Power Plant (PLTA Tanggari 1) is a hydroelectric facility that began operation in 1987, adopting vertical-type Francis turbine technology to optimize its performance. This plant is the largest renewable energy facility supporting the power system in the North Sulawesi and Gorontalo regions. The main driving source of PLTA Tanggari 1 comes from the discharge water produced by the Tonsealama Hydroelectric Power Plant. The Francis turbine-based power plant can be used for a broad spectrum of capacities, ranging from small to large scale, such as the Peusangan Hydroelectric Power Plant, which utilizes a turbine with a capacity of 23.124 MW and an efficiency of up to 93.77%.

These turbines can also be flexibly installed in either vertical or horizontal shaft configurations, depending on installation needs and maintenance accessibility. This condition often requires turbines to operate not only at the design point but also during transitions between various operating states. However, it is generally created to operate stably in single operating point, characterized by steady flow as well as minimal vortex formation at its outlet. On the other hand, operating outside the structure point leads to more intricate flow patterns as well as can trigger vortex formation at the runner outlet [11].

The Francis turbines can be operated across a broad range of heads as well as flow rates, making them the most commonly utilized turbines in hydroelectric power generation. Its main components include the spiral case (volute), stay vanes, guide vanes, runner, as well as draft tube. Its design begins with determining the power plant's flow rate and head. Each component is dimensioned and created based on these specific head as well as discharge values [12].

The Francis turbine is broadly utilized to fulfill electricity needs directly. CFD methods are highly beneficial in the turbine's design and development. However, simulating a full-scale turbine demands high-performance computing resources. Moreover, methods which are successful for one turbine may not necessarily be suitable for others. Therefore, the Francis-99 workshop was established as a forum for discussion and knowledge sharing on CFD techniques used in the field of hydroelectric power generation, particularly for high-pressure Francis turbines [2].

The HydroFlex runner is a newly designed and optimized Francis runner intended for verification as well as validation studies. This runner is designed to enable flexible operation. Meanwhile, the other turbine components—apart from the runner—remain the same as those in the Francis-99 runner configuration [13].

Most previous studies have focused on developing general mathematical models of erosion that identify the fundamental parameters influencing erosion rates. Numerous initiatives

have focused on establishing empirical relationships to forecast erosion rates for turbine runners as well as components. Nevertheless, these relationships heavily depend on constants that vary according to the specific conditions at each location. Recent improvements in CFD have been employed to simulate erosion rates along with its patterns in hydraulic turbines [14]. The operational stability of turbines is directly related to the safety of power plants [15]. Currently, the efficiency of this type of machine is around 70%, significantly lower than that of modern turbines, which can reach up to 90% [16]. Currently, the development of propeller runners is largely focused on enhancing individual capacity and boosting efficiency, which has attracted the attention of many researchers [18].

Incorporating numerical optimization algorithm into the design process proves to be a more efficient method for identifying the best final solution [19]. Enhancing the efficiency of hydraulic machinery and turbine performance has become a crucial focus within the hydraulic machinery industry [20]. A precise forecast method was developed for Francis-type turbines, calculating the entire flow field to reduce numerical errors [21]. A different method for replicating the complete turbine model involves using the flow-passage method on the distributor as well as runner domains [22]. Alongside experimental analysis, CFD simulations have also been employed to study this flow. Most of these simulations utilize Reynolds-averaged Navier–Stokes (RANS) methods due to their lower computational costs compared to scale-resolving techniques [24]. The main objective of CFD tools is to accurately estimate hydraulic efficiency and pressure distribution, while also identifying significant flow phenomena [23]. The main component, the runner, functions to convert fluid energy into mechanical energy.

To evaluate performance efficiency and extend component lifespan, a reverse engineering process was carried out on the Francis turbine runner at the Tanggari Hydroelectric Power Plant (PLTA Tanggari). The experiment objective is to analyze the design, assess performance, and identify opportunities for improvement using a Francis turbine model. This report aims to conduct reverse engineering on the Francis turbine runner at PLTA Tanggari 1, focusing on hydraulic performance analysis and geometric studies. Using 3D scanning technology and CFD simulation, this process is expected to deepen the runner design understanding as well as suggest recommendations for improving its efficiency and optimizing the design. The CFD simulation primary focus is to evaluate the water turbine's hydraulic performance, particularly the runner component, which is the core element and has the most significant impact on turbine efficiency. Through the analysis of pressure distribution and velocity profiles, the simulation aims to identify areas that may potentially cause inefficiencies or energy losses.

2. Methodology

Equation

In CFD analysis, fluid flow is analyzed using the Navier-Stokes equations, which form the fluid dynamics' foundation. These equations encompass the law of conservation of mass (continuity), momentum, and energy.

- Continuity equation:
  The continuity equation for incompressible fluids is:
  $$\frac{\partial p}{\partial t} + \nabla \cdot (\rho v) = 0$$
  Since the flow is considered incompressible (density, ρ, is constant), this equation becomes:
  $$\nabla \cdot v = 0$$
  where:
  v is the fluid velocity vector
  This equation guarantees the fluid mass in the system is conserved, with no accumulation or loss of mass within the flow domain.
- Navier-Stokes equation (Momentum):
  The momentum equation (Navier-Stokes) for fluid flow can be written as:
  $$\rho\left(\frac{\partial v}{\partial t} + v \cdot \nabla v\right) = -\nabla p + \mu \nabla^2 v + f$$
  where:
  ρ is fluid density
  p is pressure

μ is dynamic viscosity

$\boldsymbol{f}$ is the external volumetric force (gravity)

This equation shows how changes in momentum are influenced by forces such as pressure, viscous friction, and external forces. In a Francis turbine, the pressure and velocity distribution obtained from solving this equation provide insights into the runner's performance.

The flow inside a Francis turbine runner is generally turbulent, making the use of turbulence models in CFD simulations essential. The most commonly used turbulence models are the k-ε and k-ω models.

The k-ε model is a two-equation turbulence model that predicts turbulent kinetic energy (k) and the rate of turbulent energy dissipation (ϵ). The k-ε equation for turbulent kinetic energy is:

$$\frac{\partial k}{\partial t} + v \cdot \nabla k = \nabla \left(\frac{v_t}{\sigma_\epsilon} \nabla k \right) + G_k - \epsilon$$

And the equation for the rate of dissipation is:

$$\frac{\partial \epsilon}{\partial t} + v \cdot \nabla \epsilon = \nabla \left(\frac{v_t}{\sigma_\epsilon} \nabla \epsilon \right) + C_1 \frac{\epsilon}{k} G_k - C_2 \epsilon$$

where:

Gk is the production of turbulent energy

vt is the turbulent viscosity

The method used is reverse engineering. The stages of the Reverse Engineering process are as follows:

- Data Collection
  Collect the required data, including technical drawings (blueprints or original component drawings), 3D scan point clouds (from 3D scanning of the physical component), and measured dimensions (manual measurements using measuring tools).
- 3D Modeling (Casing, Guide Vane, Draft Tube)
  Create 3D models of components such as the casing (housing), guide vanes (flow directing fins), and draft tube (fluid outlet conduit).
- 3D Modeling of the Runner
  Create a 3D model of the runner (the rotating part, such as the impeller or turbine runner).
- CFD Analysis (Computational Fluid Dynamics)
  Perform fluid flow simulations using CFD methods to analyze the hydrodynamic performance of the modeled components.
- Performance Evaluation (Decision Point)
  Evaluate whether the simulated performance meets the design target or actual performance.
  - If No → Return to the "3D Modeling of the Runner" stage to revise the runner design.
  - If Yes → Proceed to the next stage.
  - Performance Curve, Hill Chart

  Once the performance is satisfactory, the analysis results are used to generate a performance curve (efficiency, head, flow rate, etc.) and a Hill chart (3D performance map for various combinations of operating parameters).
- Completion
  The reverse engineering process is considered complete.

3D Scanning

The structured light scanner utilized in 3D scanning captures the intricate geometry of the runner with great precision. The scan data, in the form of a point cloud, is processed using Spaceclaim software to produce a smooth and noise-free mesh. This mesh is then further processed into a solid CAD model that can be used for analysis.

CAD Model Creation

The CAD model is created using Spaceclaim software. This process includes converting the mesh into a solid model, smoothing the geometry, and adjusting the dimensions. The resulting CAD model is then used as the basis for CFD simulation. The main goal of 3D modeling is to obtain a 3D runner model that closely matches the actual runner's dimensions

and geometry as a reference, so that the reverse-engineered model has hydraulic performance characteristics similar to the actual runner. The process and results of 3D modeling heavily depend on the quality of the 3D scanning data acquisition.

CFD Simulation

CFD simulation was performed using ANSYS CFX to analyze the fluid flow through the runner. The boundary conditions applied include inlet flow velocity, outlet pressure, and runner wall conditions. The k-ε turbulence model was used to represent the flow under operating conditions. The simulation results were analyzed to understand the pressure distribution, fluid velocity, and flow patterns occurring inside the runner.

CFD simulation process:

- Geometry creation of the model/problem as shown in Figure 3a
- Meshing
  - Definition of the physical model:
    - k-epsilon turbulence model
    - Fluid is water with a density of 998 kg/m³
  - Pressure reference = 1 atm
  - Steady-state simulation
- The mesh in each domain is fully constructed using tetrahedral elements. Figure 1b shows the mesh for each domain. The simulation was performed without including the spiral case domain. In the numerical calculation of the turbine, the number of nodes in the spiral domain is 291,913 (elements 1,561,255), runner domain 83,869 (elements 425,865), guide vane domain 182,809 (elements 957,049), draft tube domain 44,970 (elements 231,687), with a total number of nodes of 603,561 (elements 3,175,856).

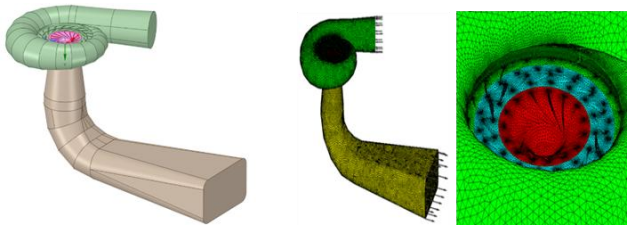

Figure 1. (a) Geometry Model of Tanggari 1 Francis Turbine for CFD Simulation (b) Meshing Domain Simulation.

Definition of Boundary Conditions

In the entire computational domain, 3D RANS equations are written in a conventional form for every mesh element. Turbulence phenomena are modeled using the k-ε model. Under the simulation operating conditions, the mass flow is specified at the spiral inlet, while an average pressure of 0 Pa is applied at the draft tube outlet. Simulations were conducted at five different guide vane opening angles (6, 11, 21, 26, 31, and 41 degrees) and at three different head levels (89.55, 122.4, and 149.4 meters). A total of 18 CFD simulation scenarios were performed The runner domain functioned as rotating domain with its axis reference at a rotation speed of 750 rpm. The process of running/solving the mathematical equations underlying the CFD was completed iteratively, analysis and visualization of the CFD solution.

3. Results and Discussion

The reverse engineering process of the runner begins with acquiring 3D scanning data of the runner as shown in Figure 2. The 3D scan data is used as a geometric reference in the 3D modeling of the runner. The 3D model obtained through the reverse engineering process is then verified in terms of hydraulic performance and structural strength using CFD analysis. The 3D modeling is carried out using SpaceClaim software, while the CFD analysis is performed using ANSYS CFX.

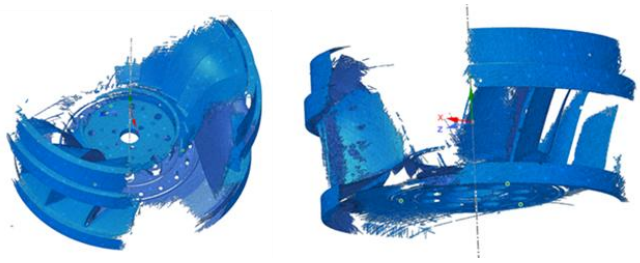

Figure 2. Runner of Tanggari 1 Hydropower Plant from 3D scanning results.

Re-modeling Results

The reference surface model data cannot be directly used as a reference during the 3D model reconstruction process because the data must go through filtering, removing, and alignment processes to facilitate the reconstruction of the blades and ensure conformity with the reference coordinates. In the reconstruction process, at least three features must match the reference data, namely the blades, hub, and shroud. Figure 3 shows the 3D model of the PLTA Tanggari 1 runner after remodeling.

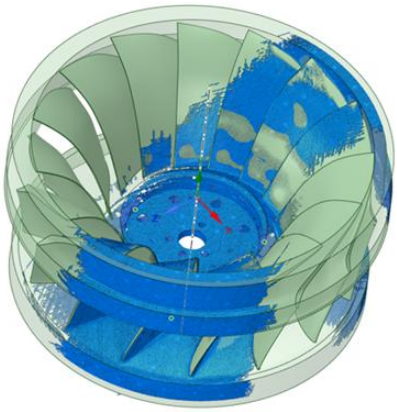

Figure 3. 3D model of the Tanggari 1 Hydropower Plant runner after remodelling.

CFD Simulation Results

Turbine Performance Curve

Table 1 shows the turbine performance parameter values obtained from the CFD simulation. The CFD simulations were performed at five guide vane opening angles, namely 6, 11, 21, 26, 31, and 41 degrees, with head variations of 89.5, 122.4, and 149.4 meters. The turbine's flow rate varies based on the head and the angle of the guide vane opening. The guide vanes (GV) in Francis turbines experience intermittent flow effects as a result of high flow velocities and rapid accelerations [26]. According to Brekke, the wakes generated by the guide vanes in a Francis turbine behave like 'pressure shock' waves, inducing strong pressure pulsations within the runner [27]. The guide vane configurations that were developed align with the earlier geometric descriptions and flow analysis. These configurations rely on turbine input parameters, which play a vital role in the preliminary design phase [28]. IGVs positioned at 0° were found to have negligible influence on the pump's hydraulic behavior in both high-efficiency regions and at low flow rates [29]. This impact the pressure distribution causing flow separation on the blades [12].

Table 1. Performance of Francis Turbine at PLTA Tanggari 1 from Simulation Results.

Head 89.5 meter			
Guide vane angle (degrees)	**Discharge (m^3/s)**	**Axle Power (MW)**	**Efficiency (%)**
6	1.43	0.27	0.21
11	2.76	1.65	0.67
21	5.67	4.318	0.865
26	6.9	5.33	0.88
31	8.03	6.27	0.89

41	9.27	6.11	0.76
Head 122.4 meter			
Guide vane angle (degrees)	**Discharge (m³/s)**	**Axle Power (MW)**	**Efficiency (%)**
6	1.7433	1.079	0.515
11	3.3859	3.207	0.79
21	6.93	7.614	0.917
26	8.4662	9.5282	0.9398
31	9.66	10.616	0.9195
41	11.59	11.85	0.855
Head 149.4 meter			
Guide vane angle (degrees)	**Discharge (m³/s)**	**Axle Power (MW)**	**Efficiency (%)**
6	1.974	1.764	0.61
11	3.88	4.59	0.8
21	7.88	10.68	0.9255
26	9.4255	12.64	0.9185
31	10.8	14.28	0.904
41	12.82	15.5	0.833

At a head of 122.4 meters (the actual head level at which the turbine operates in PLTA Tanggari 1), the maximum output power is achieved at the largest guide vane opening (guide vane angle of 41°) with a shaft power of 11.85 MW. At this level, the maximum efficiency of 93% is reached at a guide vane opening of 26°, with a turbine shaft output power of 9.53 MW at an inlet flow rate of 8.5 m³/s.

The graph in Figure 4 is a performance curve that shows the flow rate (guide vane opening) influence on the turbine operating parameters (power and efficiency) at each different head level. The water's flow rate increases as the guide vane opening becomes larger. The pattern of increasing shaft output power shows a comparable trend to the increasing flow rate as the guide vane opening widens. The performance curve pattern at each head level tends to be the same, where turbine efficiency increases as the flow rate entering the turbine rises (achieved by increasing the guide vane opening) until reaching the best efficiency point (BEP), then decreases as the guide vane opening continues to increase.

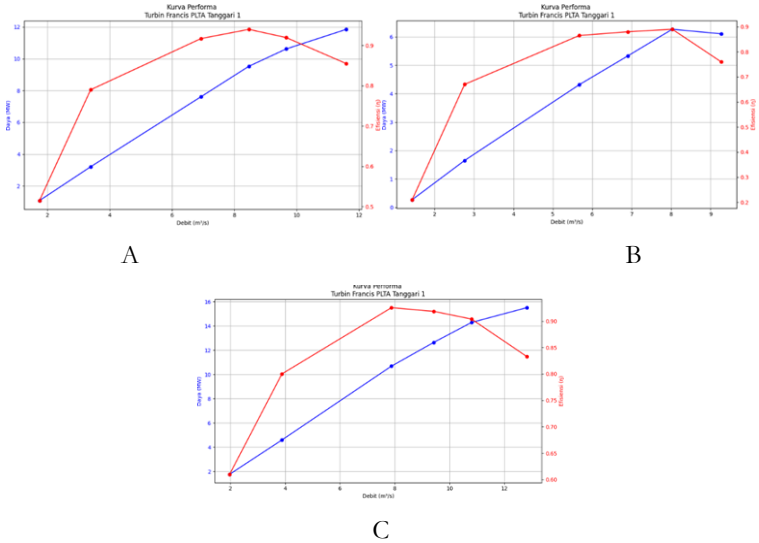

A B C

Figure 4. Performance curve at (a) head 89.5 meter (b) head 122.4 meter (c) head 149.4 meter.

In the curve shown in Figure 4, where the turbine operates at a head level of 122.4 meters, the turbine reaches its peak efficiency at a specific flow rate. The peak efficiency from the simulation results for the Francis turbine at PLTA Tanggari 1 is 93%. When flow rates are below or above this point, turbine efficiency declines. This curve is parabolic in shape, with efficiency peaking in the middle and decreasing on both sides at low and high flow rates. At highest efficiency, the flow rate entering the turbine is called the nominal flow rate, and

this condition is referred to as BEP. The flow percentage is represented by the guide vane opening angle, with 100% flow aligning with the best efficiency point [30].

Hill Chart

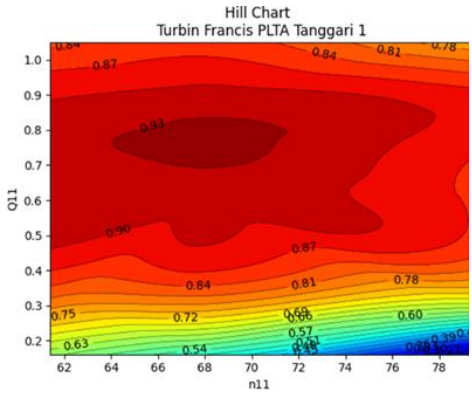

Figure 2. Hill chart francis turbine PLTA Tanggari 1

A Hill chart is a graphical representation used to illustrate the correlation between flow rate (Q), head (H), rotational speed (rpm), runner dimensions (D), and the hydraulic turbine efficiency such as a Francis turbine. The Hill chart displays efficiency contours in the form of hills, where the peaks indicate the optimal conditions for combinations of flow rate, rotational speed, and head that yield the highest efficiency.

These contour lines guide turbine operators in understanding how changes in flow rate and head affect turbine performance, thereby assisting in operational adjustments to ensure the turbine works at maximum efficiency. This is useful for monitoring, optimizing, and planning turbine operations more effectively. The Hill chart of the Francis turbine at PLTA Tanggari 1 is shown in Figure 5.

$$n_{11} = \frac{nD}{\sqrt{H}} \; ; \; Q_{11} = \frac{Q}{D^2\sqrt{H}}$$

n11 is the value of the unit speed and Q11 is the unit flow rate value, both calculated using the equations above. Where, n represent the rotational speed, D stands for the runner diameter, and H refers to the turbine head. The efficiency values and other parameters obtained from the CFD simulations are used to calculate the n11 and Q11 values for each turbine operating condition, which are then plotted on the Hill chart graph.

Pressure Contours

Figures 6–8 show the water pressure contours on the runner, where the pressure values gradually decrease from the inlet to outlet. At the outlet, the water pressure on the runner diminishes because the water pressure is converted into mechanical torque work by the runner blades. The figures also show a pressure discrepancy between the turbine blades' pressure and suction side. This pressure difference generates a force on the runner blades, producing torque on the runner shaft.

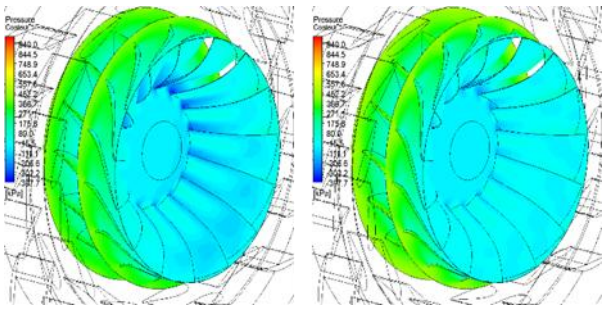

GV 6° Angle GV 11° Angle

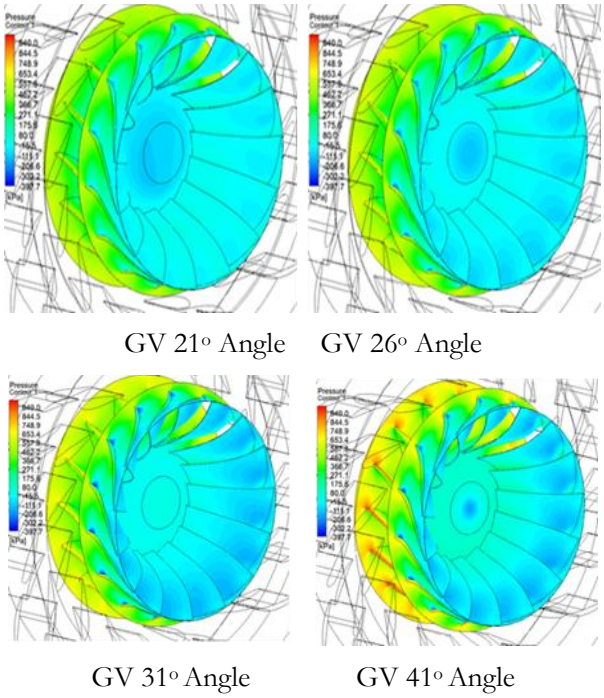

Figure 6. Runner pressure contours at operating head of 89 meters.

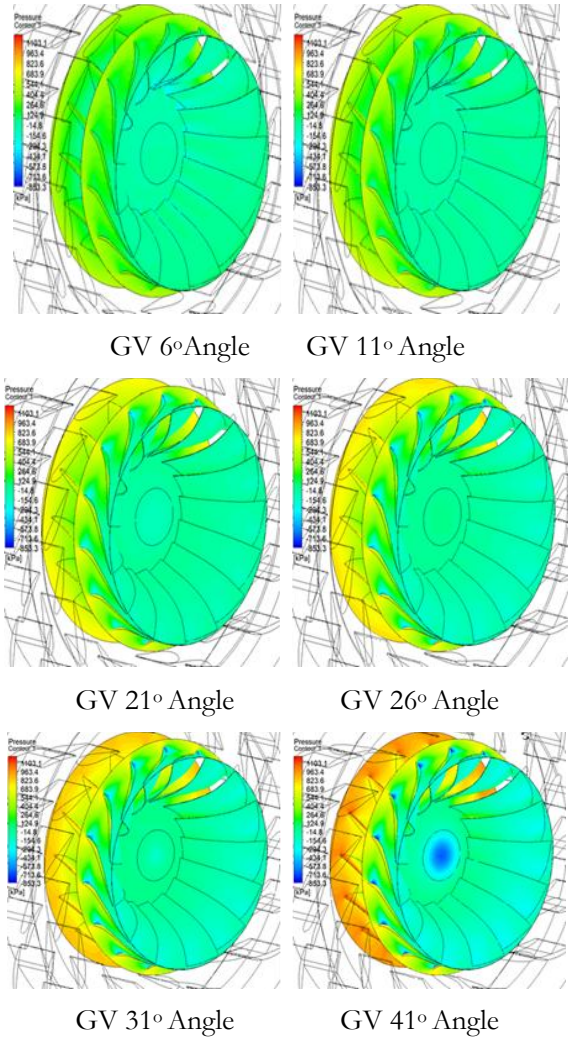

Figure 7. Runner pressure contours at an operating head of 122 meters.

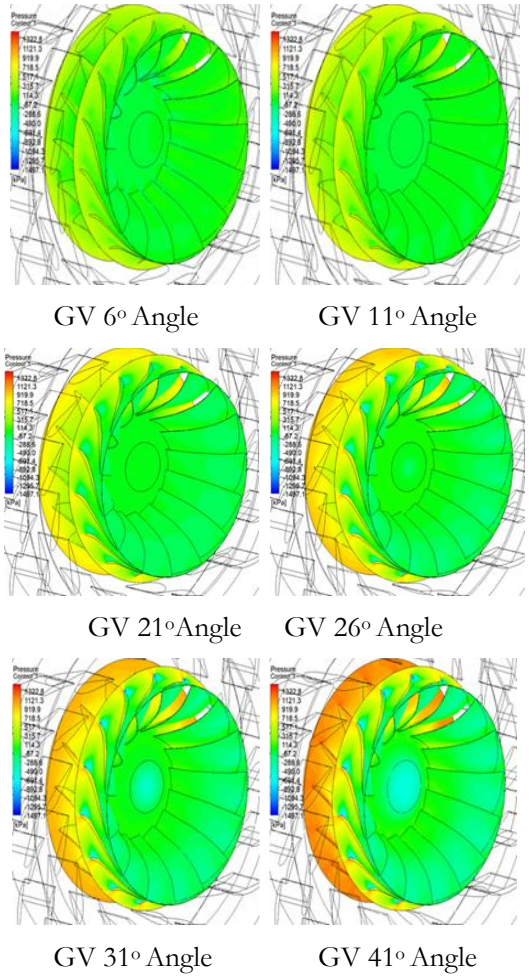

GV 6° Angle GV 11° Angle

GV 21°Angle GV 26° Angle

GV 31° Angle GV 41° Angle

Figure 8. Runner pressure contours at an operating head of 149 meters.

Fluid Flow (Streamline)

The fluid flow in the runner and draft tube is shown in Figures 9–11. At the optimum guide vane opening angle, where the turbine efficiency is highest, the flow in the runner occurs as expected according to the design conditions, without flow separation or vortex flow in the runner. At medium openings, only minor secondary flow occurs in the suction side area of the blades near the hub. Flow separation occurs at small guide vane openings (low flow rate) around the suction side of the blades, marked by vortex flow in the space between the runner blades. This flow also causes local pocket pressure in the blade passage. The vortex flow phenomenon in the runner affects the dynamic pressure on the runner. The greater the pressure fluctuates, the higher the vibration on the runner.

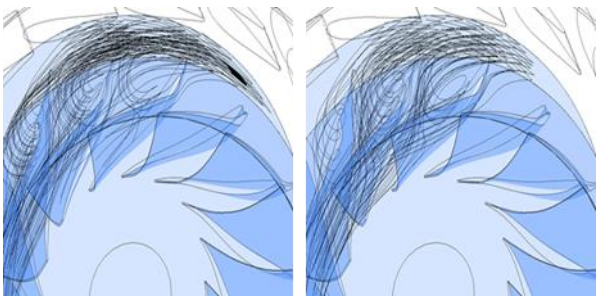

GV 6° Angle GV 11° Angle

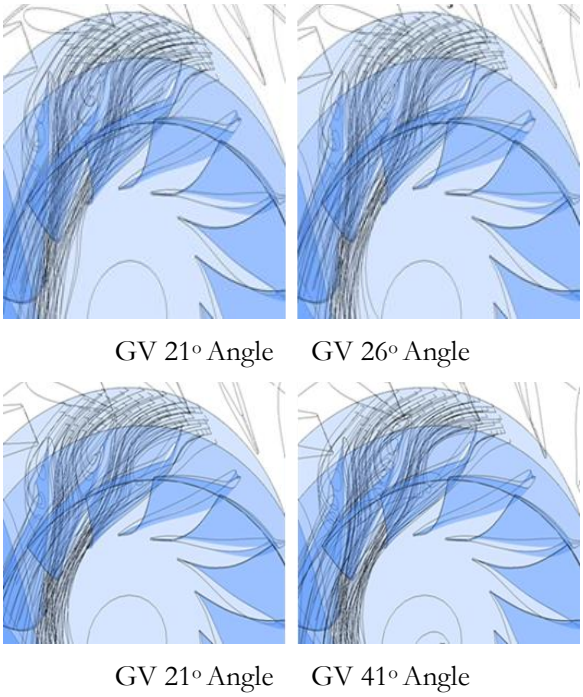

Figure 9. Water flow in the runner at an operating head of 89 meters.

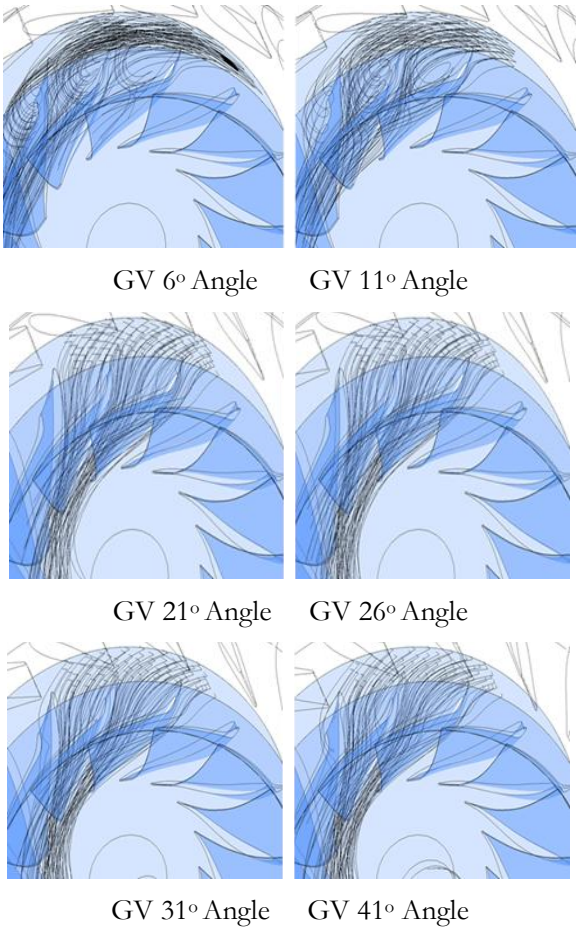

Figure 10. Water flow in the runner at an operating head of 122 meters.

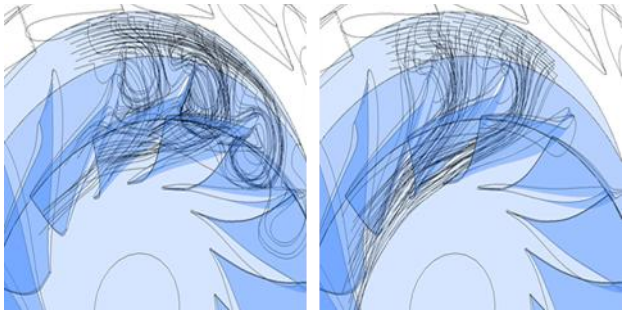

(a) GV 6° Angle (b) GV 11° Angle

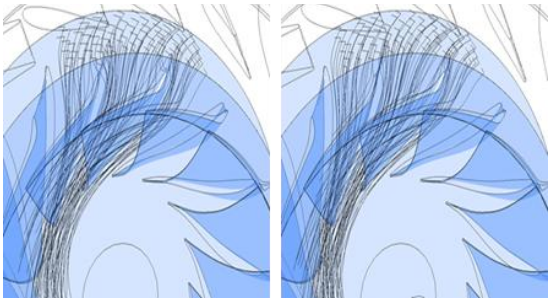

(c) GV 21° Angle (d) GV 26° Angle

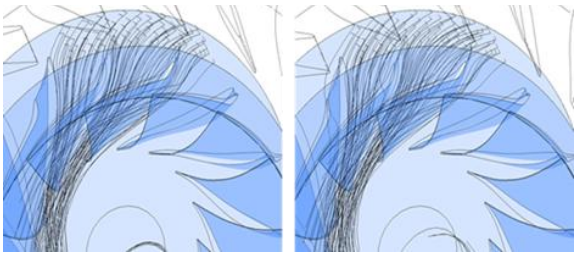

(e) GV 31° Angle (f) GV 41° Angle

Figure 11. Water flow in the runner at an operating head of 149 meters.

Swirling flow in the draft tube occurs at partial loads (below 50% and above 110% of the nominal flow rate). The water flow patterns passing through the draft tube are shown in Figures 12–14. At medium/optimum openings (around the nominal flow rate), the water flow in the draft tube is relatively parallel to the draft tube axis. Similar to the secondary flow and separation in the runner, the swirling flow in the draft tube also affects the flow dynamics in the draft tube, which impacts turbine vibrations.

At openings with flow rates below 50% and above 110%, although swirling flow occurs in both cases, the direction of swirling flow in the draft tube differs. At flow rates below 50%, the swirling direction is opposite to the runner's rotation, whereas at flow rates above 110%, the swirling flow direction is the same as the runner's rotation.

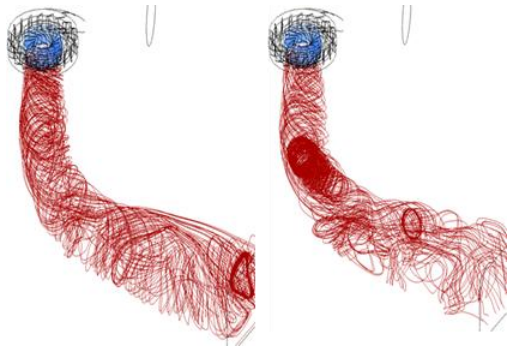

GV 6° Angle GV 11° Angle

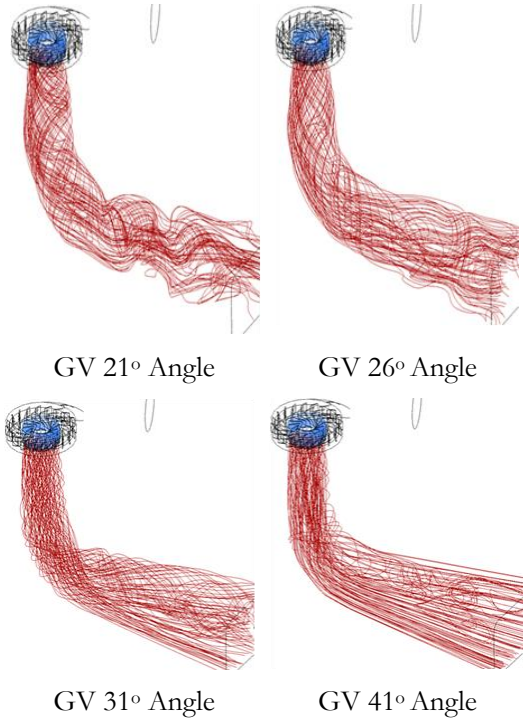

Figure 12. Water flow in the draft tube at an operating head of 89 meters.

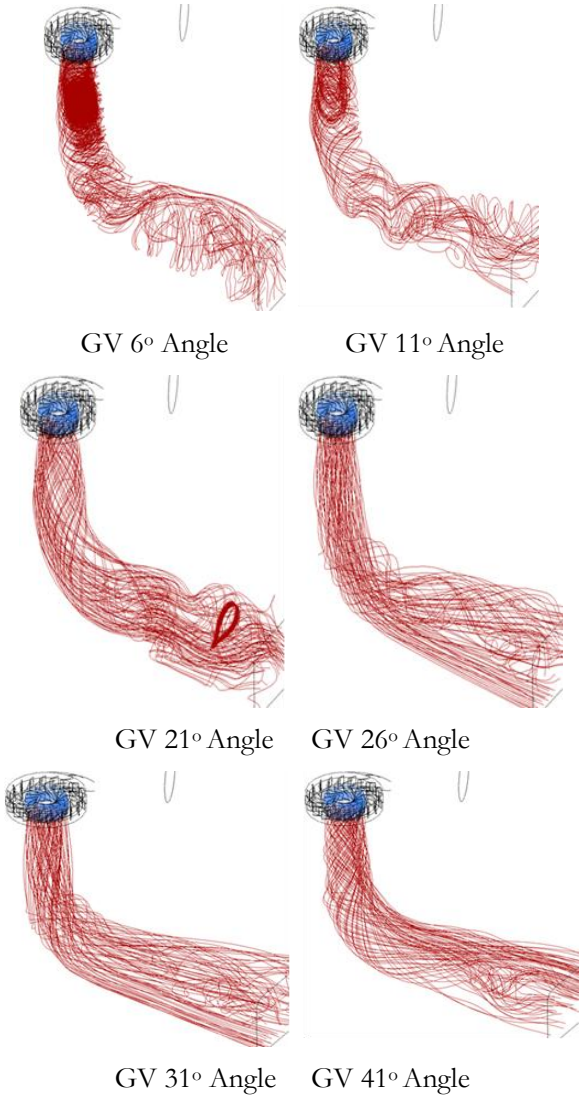

Figure 13. Water flow in the draft tube at an operating head of 122 meters.

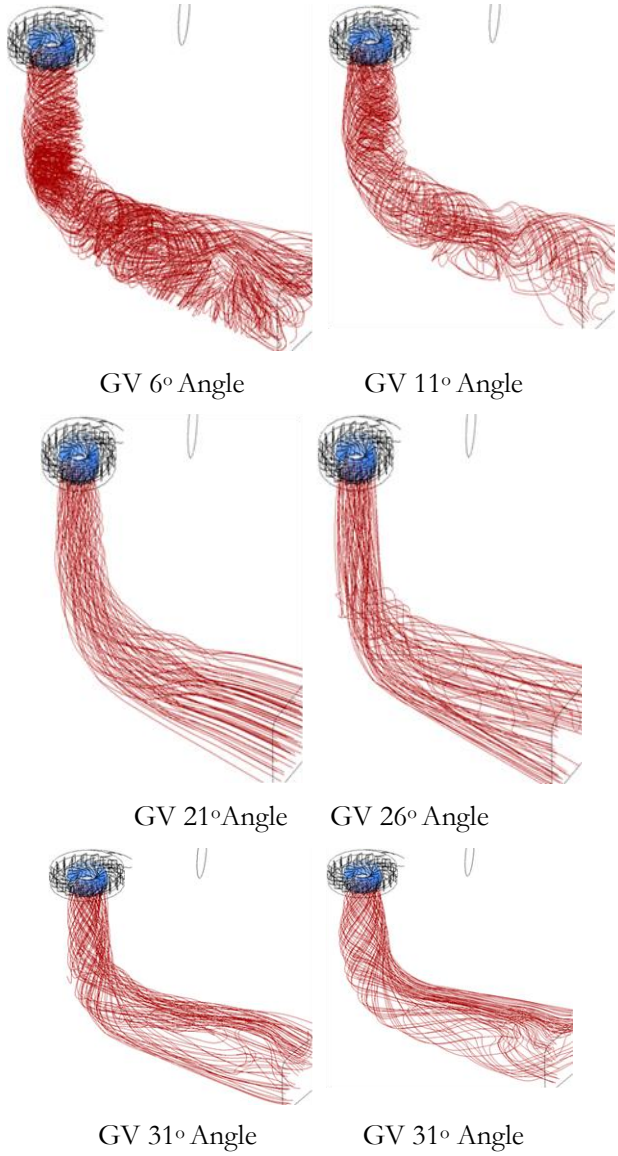

Figure 14. Water flow in the draft tube at an operating head of 122 meters.

4. Conclusions

This study successfully conducted reverse engineering on the Francis turbine runner of the Tanggari 1 Hydroelectric Power Plant by utilizing 3D scanning technology and Computational Fluid Dynamics (CFD) simulation. The remodeled runner showed good geometric conformity with the original component. CFD simulations indicated that the turbine's maximum efficiency reached 93% at a head of 122.4 meters with a guide vane opening angle of 26° and a flow rate of 8.5 m^3/s.

The performance curve and hill chart generated from the simulations revealed a Best Efficiency Point (BEP), which is crucial for optimizing turbine operation. Pressure distribution and flow patterns on the runner showed that optimal flow occurs at a medium guide vane opening. Conversely, at small and large openings, flow separation and vortex phenomena were identified, causing pressure fluctuations and increased vibrations in the runner.

Overall, the reverse engineering approach combined with CFD simulation proved effective in analyzing and improving turbine performance. The results of this study can serve as a basis for runner design improvements and more efficient turbine operation management in the future.

Author Contributions: "Conceptualization: Achmad Walid and Irwanda Yuni Pungkiarto; Methodology: Irwanda Yuni Pungkiarto; Software: Irwanda Yuni Pungkiarto; Validation: Achmad Walid, Irwanda Yuni Pungkiarto; Formal analysis: Achmad Walid; Investigation: Achmad Walid; Resources: Irwanda Yuni Pungkiarto; Data curation: Achmad Walid; Writing—original draft preparation: Achmad Walid; Writing—review and editing: Achmad Walid;

Visualization: Irwanda Yuni Pungkiarto; Supervision: Achmad Walid ; Project administration: Achmad Walid; Funding acquisition:Irwanda Yuni Pungkiarto."

Funding:"This research received no external funding"

Data Availability Statement: We encourage all authors of articles published in FAITH journals to share their research data.

Acknowledgments: We acknowledge any support from State Polytechnic of Malang.

Conflicts of Interest: The authors declare no conflict of interest".

References

[1] F. Ayancik, C. Kutay, and A. Selin, "Parametrical and theoretical design of a Francis turbine runner," in *Proc. HEFAT2014 10th Int. Conf. Heat Transfer, Fluid Mechanics and Thermodynamics*, Orlando, FL, Jul. 2014, pp. 775–780.

[2] C. Trivedi and M. J. Cervantes, "State of the art in numerical simulation of high head Francis turbines," *Renew. Energy Environ. Sustain.*, vol. 20, pp. 10–14, 2016, doi: 10.1051/rees/2016032.

[3] D. Zhu, R. Xiao, R. Tao, and W. Liu, "Impact of guide vane opening angle on the flow stability in a pump-turbine in pump mode," *Proc. Inst. Mech. Eng. Part C: J. Mech. Eng. Sci.*, vol. 0, no. 0, pp. 1–9, 2016, doi: 10.1177/0954406216635204.

[4] E. Science, "Experimental and CFD simulation validation performance analysis of Francis turbine," *IOP Conf. Ser.: Earth Environ. Sci.*, vol. 1037, 2022, doi: 10.1088/1755-1315/1037/1/012003.

[5] H. Choi *et al.*, "CFD validation of performance improvement of a 500 kW Francis turbine," *Renew. Energy*, vol. 54, pp. 111–123, 2013, doi: 10.1016/j.renene.2012.08.049.

[6] E. Ayli, K. Celebioglu, and S. Aradag, "Mechanics determination and generalization of the effects of design parameters on Francis turbine runner performance," *Eng. Appl. Comput. Fluid Mech.*, vol. 10, no. 1, pp. 547–566, 2016, doi: 10.1080/19942060.2016.1213664.

[7] D. R. Dahal *et al.*, "A simplified Francis turbine for micro hydro application: Design and numerical analysis," *IOP Conf. Ser.: Earth Environ. Sci.*, vol. 627, 2021, doi: 10.1088/1755-1315/627/1/012018.

[8] Z. Tong *et al.*, "Investigating the performance of a super high-head Francis turbine under variable discharge conditions using numerical and experimental approach," *Energies*, vol. 13, no. 15, p. 3868, 2020, doi: 10.3390/en13153868.

[9] K. Rozi *et al.*, "Experimental study on performance of a hydraulic Francis turbine with variations of runner speed," *Int. Res. J. Innov. Eng. Technol. (IRJIET)*, vol. 8, no. 5, pp. 82–88, 2024.

[10] F. Ayancik *et al.*, "Hydroturbine runner design and manufacturing," *Int. J. Mater. Mech. Manuf.*, vol. 1, no. 2, pp. 162–165, 2013, doi: 10.7763/IJMMM.2013.V1.35.

[11] L. Stoessel, "Steady and unsteady numerical simulations of the flow in the Tokke Francis turbine model, at three operating conditions," *J. Phys.: Conf. Ser.*, vol. 579, 2021, doi: 10.1088/1742-6596/579/1/012011.

[12] K. Celebioglu and F. Z. A. Yilmaz, "Numerical investigation of the effects of design parameters on hydraulic turbine guide vane design," *Pamukkale Univ. J. Eng. Sci.*, vol. 26, no. 4, pp. 666–673, 2020, doi: 10.5505/pajes.2019.70850.

[13] C. Trivedi, I. Iliev, and O. G. Dahlhaug, "Numerical study of a Francis turbine over wide operating range: Some practical aspects of verification," *Sustainability*, vol. 12, no. 10, p. 4301, 2020, doi: 10.3390/su12104301.

[14] B. Singh, B. Thapa, and O. G. Dahlhaug, "Empirical modelling of sediment erosion in Francis turbines," *Energy*, vol. 41, no. 1, pp. 386–391, 2012, doi: 10.1016/j.energy.2012.02.066.

[15] M. S. G. Tsuzuki *et al.*, "Development of a complete methodology to reconstruct, optimize, analyze and visualize Francis turbine runners," *IFAC-Pap. OnLine*, vol. 3, pp. 1900–1905, 2015, doi: 10.1016/j.ifacol.2015.06.364.

[16] L. A. Teran, F. Jose, and S. A. Rodriguez, "Performance improvement of a 500-kW Francis turbine based on CFD," *Renew. Energy*, vol. 96, 2016, doi: 10.1016/j.renene.2016.05.044.

[17] A. Cerriteno *et al.*, "Reconstruction of the Francis 99 main runner blade using a hybrid parametric approach," *IOP Conf. Ser.: Earth Environ. Sci.*, vol. 774, no. 1, p. 012074, 2021, doi: 10.1088/1755-1315/774/1/012074.

[18] L. Youyu *et al.*, "Digital hydraulic design for low-specific-speed propeller runners with fixed blades," *Symmetry*, vol. 14, no. 11, p. 2250, 2022, doi: 10.3390/sym14112250.

[19] S. Thum and R. Schilling, "Optimization of hydraulic machinery bladings by multilevel CFD techniques," *Int. J. Rotating Mach.*, vol. 2, no. 2, pp. 161–167, 2025, doi: 10.1155/IJRM.2005.161.

[20] F. Ayancik, K. Celebioglu, and S. Aradag, "Parametrical and theoretical design of a Francis turbine runner with the help of computational fluid dynamics," in *Proc. HEFAT2014 10th Int. Conf. Heat Transfer, Fluid Mechanics and Thermodynamics*, Jul. 2014, pp. 775–780.

[21] E. Ayli, K. Celebioglu, and S. Aradag, "Mechanics determination and generalization of the effects of design parameters on Francis turbine runner performance," *Eng. Appl. Comput. Fluid Mech.*, pp. 545–564, 2016, doi: 10.1080/19942060.2016.1213664.

[22] J. Joy, M. J. Cervantes, and M. Raisee, "Reduced numerical modeling of a high head Francis turbine draft tube at part load," *Int. J. Fluid Mach. Syst.*, vol. 14, no. 1, Jan.–Mar. 2021, doi: 10.5293/IJFMS.2021.14.1.095.

[23] H. Wallimann and R. Neubauer, "Numerical study of a high head Francis turbine with measurements from the Francis-99 project," *J. Phys.: Conf. Ser.*, vol. 579, p. 012003, 2015, doi: 10.1088/1742-6596/579/1/012003.

[24] M. H. Arabnejad, H. Nilsson, and E. B. Rickard, "Investigation of flow-induced instabilities in a Francis turbine operating in non-cavitating and cavitating part-load conditions," *Fluids*, vol. 8, no. 2, 2023, doi: 10.3390/fluids8020061.

[25] R. Lama *et al.*, "Development of a test rig for investigating the performance of a model Francis turbine," *IOP Conf. Ser.: Earth Environ. Sci.*, vol. 1079, 2022, doi: 10.1088/1755-1315/1079/1/012011.

[26] R. K. Sahu, B. K. Gandhi, and S. Sharma, "Numerical flow field investigation around guide vane of a high head Francis turbine," *J. Phys.: Conf. Ser.*, 2023, doi: 10.1088/1742-6596/2629/1/012001.

[27] S. Chitrakar, B. S. Thapa, O. G. Dahlhaug, and H. P. Neopane, "Numerical investigation of the flow phenomena around a low specific speed Francis turbine's guide vane cascade," *Eng. Appl. Comput. Fluid Mech.*, vol. 49, p. 062016, 2016, doi: 10.1080/19942060.2018.1509806.

[28] F. Stojkovski *et al.*, "Constraints of parametrically defined guide vanes for a high-head Francis turbine," *Energies*, vol. 14, no. 9, 2021, doi: 10.3390/en14092667.

[29] H. Jiao, C. Sun, and S. Chen, "Analysis of the influence of inlet guide vanes on the performance of shaft tubular pumps," *Shock Vib.*, vol. 5177313, p. 17, 2021, doi: 10.1155/2021/5177313.

[30] R. Lama *et al.*, "Numerical investigation on performance and sediment erosion of Francis runner with different guide vane profiles," *J. Phys.: Conf. Ser.*, vol. 1042, pp. 012004, 2018, doi: 10.1088/1742-6596/1042/1/012004.